CI&CEQ

Available on line at
Association of the Chemical Engineers of Serbia *AChE*
www.ache.org.rs/CICEQ

Chemical Industry & Chemical Engineering Quarterly 18 (3) 483–493 (2012) CI&CEQ

S. SRINIVAS[1]
R. MUTHURAJ[2]
J. SAKINA[1]

[1]Fluid Dynamics Division, School of Advanced Sciences, VIT University, Vellore, India
[2]Department of Mathematics, P.S.N.A. College of Engineering and Technology, Dindigul, India

SCIENTIFIC PAPER

UDC 532:544:66

DOI 10.2298/CICEQ111213028S

A NOTE ON THE INFLUENCE OF HEAT AND MASS TRANSFER ON A PERISTALTIC FLOW OF A VISCOUS FLUID IN A VERTICAL ASYMMETRIC CHANNEL WITH WALL SLIP

This note deals with the influence of heat and mass transfer on peristaltic flow of a viscous fluid with wall slip condition. The flow is investigated in a wave frame of reference moving with the velocity of the wave. The channel asymmetry is produced by choosing the peristaltic wave train on the walls to have different amplitude and phase. The momentum and energy equations have been linearized under the assumption of long-wavelength approximation. The arising equations are solved by perturbation technique and the expressions for temperature, concentration, velocity and stream function are constructed. Graphical results are sketched for various embedded parameters and discussed in detail.

Keywords: mixed convection; peristaltic flow; asymmetric channel; wall slip; Dufour number; Schmidt number.

Mixed convection flow in a vertical channel has received considerable attention for its possible application in many industrial and engineering processes. In modern electronic devices, particularly, circuit density as well as power dissipation of electronic components have become very large due to advances of current technology, which may result in overheating of the system. Therefore, large amounts of heat must be carried away by a suitable method in order to maintain reliable performance and long life of the system. In view of applications, several theoretical investigations have been made just to understand mixed convection in fluid flow [1-3]. Later, Chamkha *et al.* [4] have presented both analytical and numerical results of the problem of fully developed free convection flow of a micropolar fluid between a parallel-plate vertical channel with asymmetric wall temperature distribution. Prathap Kumar *et al.* [5] have analyzed the problem of fully developed combined free and forced convective flow in a fluid saturated porous medium channel bounded by two vertical parallel plates. Pop *et al.* [6] have investigated the steady fully developed mixed convection flow in a vertical channel with constant temperature walls when there is a heat generated by an exothermic reaction inside the channel. Muthuraj and Srinivas [7] have studied mixed convective heat and mass transfer in a vertical wavy porous space with traveling thermal waves.

Peristaltic flow is generated when the progressive wave travels along the wall of the tube. The studies of peristaltic flows of Newtonian and non-Newtonian fluids occurs widely in functioning of ureter, transport of bile, transport of cilia, vaso motion of small blood vessels etc. Moreover, by using the principle of peristalsis, some biomechanical instruments, e.g. heart-lung machine, have been fabricated [11]. Hayat and Hina [27] have studied the influence of wall properties on the MHD peristaltic flow of a Maxwell fluid with heat and mass transfer. Nadeem and Akbar [28] have discussed the influence of radially varying MHD on the peristaltic flow in an annulus with heat and mass transfer. Srinivas *et al.* [29] have examined the mixed convective heat and mass transfer in an asymmetric channel with peristalsis. More recently, Srinivas and Muthuraj [30] have investigated the effects of chemical reaction and space porosity on MHD mixed convective peristaltic flow in a vertical asymmetric channel. Some relevant works on the topic are given in Refs [8-35]. Nearly 200 years ago, Navier [36] proposed a general boundary

Correspondening author: S. Srinivas, Fluid Dynamics Division, School of Advanced Sciences, VIT University, Vellore - 632 014, India.
E-mail: srinusuripeddi@hotmail.com
Paper received: 13 December, 2011
Paper revised: 26 March, 2012
Paper accepted: 29 March, 2012

condition that permits the possibility of fluid slip at a solid boundary. This boundary condition assumes that the tangential velocity of the fluid relative to the solid at a point on its surface is proportional to the tangential stress acting at that point. The constant of proportionality between these two quantities may be termed as a coefficient of sliding friction, it is assumed to depend only on the nature of the fluid and solid surface [37]. Later, there has been an increase of interest in studying fluid problems with slip boundary conditions [38-46]. Ebaid [44] studied the effects of magnetic field and wall slip conditions on the peristaltic transport of a Newtonian fluid in an asymmetric channel. Srinivas *et al.* [45] have discussed the influence of slip conditions, wall properties and heat transfer on MHD peristaltic transport. Most recently, Srinivas and Muthuraj [46] also analyzed the MHD flow with slip effects and temperature dependent heat source in a vertical wavy porous space.

To the best of our knowledge the influence of heat and mass transfer on peristaltic flow in a vertical asymmetric channel with slip effect has not been studied before. The slip boundary condition would be most useful for certain problems in chemical engineering. It is a useful model for some flows through pipes in which chemical reaction occurs at the walls, for flows with laminar film condensation, for certain two-phase flows and for flows in porous slider bearings ([46] and references therein). Hence, the main objective of this investigation is to study the mixed convective heat and mass transfer flow in a vertical asymmetric channel with peristalsis and wall slip condition. The momentum and energy equations have been linearized under long-wavelength approximation and the analytic solutions for flow variables are constructed. Graphs are presented to illustrate the significance of the key parameters on the velocity, temperature and concentration distributions.

Mathematical model

Consider an incompressible viscous fluid filling a two-dimensional vertical channel. The sinusoidal waves propagating along the channel walls are of the following forms:

$$H_1 = d_1 + a_1 \cos\frac{2\pi}{\lambda}(X - ct) \text{ - right hand side wall and}$$

$$H_2 = -d_2 - b_1 \cos\left(\frac{2\pi}{\lambda}(X - ct) + \varphi\right) \text{ -}$$

left hand side wall (1)

In Eq. (1), a_1, b_1 are the amplitudes of the waves, λ is the wave length, $d_1 + d_2$ is the width of the channel, φ, $0 \le \varphi \le \pi$, is the phase difference. Note that $\varphi = 0$ corresponds to symmetric channel with waves out of phase and $\varphi = \pi$ the waves are in phase. Further a_1, b_1, d_1, d_2 and φ satisfies the condition:

$$a_1^2 + b_1^2 + 2a_1 b_1 \cos\varphi \le (d_1 + d_2)^2 \quad (2)$$

The temperature at the right hand side wall is T_0 and concentration is C_0 while the temperature at the left hand side wall is T_1 and concentration is C_1 (see flow geometry in Figure 1).

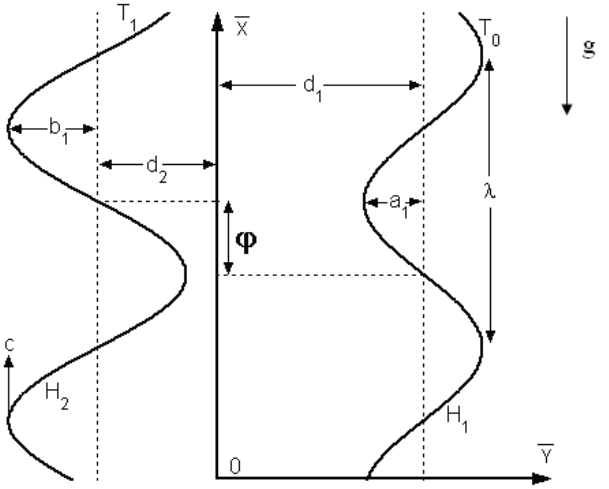

Figure 1. Schematic diagram of the physical model.

In the laboratory frame governing equations are:

$$\frac{\partial U}{\partial X} + \frac{\partial V}{\partial Y} = 0 \quad (3)$$

$$\rho\left[\frac{\partial U}{\partial t} + U\frac{\partial U}{\partial X} + V\frac{\partial U}{\partial Y}\right] = -\frac{\partial P}{\partial X} + \mu\left(\frac{\partial^2 U}{\partial X^2} + \frac{\partial^2 U}{\partial Y^2}\right) + \rho g\beta_t(T - \overline{T}) + \rho g\beta_c(C - \overline{C}) \quad (4)$$

$$\rho\left[\frac{\partial V}{\partial t} + U\frac{\partial V}{\partial X} + V\frac{\partial V}{\partial Y}\right] = -\frac{\partial P}{\partial Y} + \mu\left(\frac{\partial^2 V}{\partial X^2} + \frac{\partial^2 V}{\partial Y^2}\right) \quad (5)$$

$$\left[\frac{\partial T}{\partial t} + U\frac{\partial T}{\partial X} + V\frac{\partial T}{\partial Y}\right] = \frac{k}{\rho c_p}\left[\frac{\partial^2 T}{\partial X^2} + \frac{\partial^2 T}{\partial Y^2}\right] + \frac{D_m k_T}{c_s c_p}\left(\frac{\partial^2 C}{\partial X^2} + \frac{\partial^2 C}{\partial Y^2}\right) \quad (6)$$

$$\left[\frac{\partial C}{\partial t} + U\frac{\partial C}{\partial X} + V\frac{\partial C}{\partial Y}\right] = D_m\left[\frac{\partial^2 C}{\partial X^2} + \frac{\partial^2 C}{\partial Y^2}\right] + \frac{D_m k_T}{\overline{T}}\left(\frac{\partial^2 T}{\partial X^2} + \frac{\partial^2 T}{\partial Y^2}\right) \quad (7)$$

where U, V are the velocity components in X and Y direction respectively, g is the acceleration due to gravity, T is the temperature of the fluid, C is the concentration of the fluid, $\overline{T}$ is the temperature at

some reference point, $\overline{C}$ is the concentration at some reference point, ρ is density of fluid, μ is dynamic viscosity of the fluid, P is the pressure, β_t is the coefficient of thermal expansion, β_c is the coefficient of expansion with concentration, c_p is the specific heat at constant pressure, D_m is the coefficient of mass diffusivity, k is the thermal conductivity, k_T is the thermal-diffusion ratio and c_s is the concentration susceptibility. In writing the above equations the following assumptions are made: *i*) the Boussinesq approximation is invoked so that the density variations will be retained only in the buoyancy term and *ii*) the dissipation function effect is neglected.

Under the assumptions stated above, we shall investigate a coordinate system, moving with the wave speed *c*, in which the boundary shape is stationary. Defining in wave frame (x, y), the velocity components (u, v) and pressure p by:

$$x = X - ct,\ y = Y,\ u = U - c,\ v = V,\ p(x) = P(X,t) \quad (8)$$

Introducing the following non-dimensional quantities:

$$\begin{aligned}
&\bar{x} = \frac{x}{\lambda};\ \bar{y} = \frac{y}{d_1};\ \bar{u} = \frac{u}{c};\ \bar{v} = \frac{v}{c\delta};\ \delta = \frac{d_1}{\lambda};\ \bar{p} = \frac{d_1^2 p}{\mu c \lambda};\\
&\bar{t} = \frac{ct}{\lambda};\ h_1 = \frac{H_1}{d_1};\ h_2 = \frac{H_2}{d_1};\ d = \frac{d_2}{d_1};\ a = \frac{a_1}{d_1};\ b = \frac{b_1}{d_1}\\
&\mathrm{Re} = \frac{\rho c d_1}{\mu};\ \theta = \frac{T - \overline{T}}{T_0 - \overline{T}};\ n = \frac{T_1 - \overline{T}}{T_0 - \overline{T}};\ \phi = \frac{C - \overline{C}}{C_0 - \overline{C}};\\
&m = \frac{C_1 - \overline{C}}{C_0 - \overline{C}};\ P_r = \frac{c_p \mu}{k};\ S_c = \frac{\mu}{\rho D_m};\\
&D_f = \frac{\rho D_m k_T (C_0 - \overline{C})}{c_s c_p (T_0 - \overline{T})\mu};\ S_r = \frac{\rho D_m k_T (T_0 - \overline{T})}{\overline{T}(C_0 - \overline{C})\mu};\\
&g_t = \frac{\rho g \beta_t \left(T_0 - \overline{T}\right) d_1^2}{\mu c};\ g_c = \frac{\rho g \beta_c \left(C_0 - \overline{C}\right) d_1^2}{\mu c}
\end{aligned} \quad (9)$$

where Re is the Reynolds number, δ is the dimensionless wave number, g_t is the local temperature Grashof number, g_c is the local mass Grashof number, P_r is the Prandtl number, S_c is the Schmidt number, D_f is the Dufour number, S_r is the Soret number. Invoking the above non-dimensional variables, the basic field Eqs. (3)-(7) can be expressed in the non-dimensional form, dropping the bars:

$$\frac{\partial u}{\partial x} + \frac{\partial v}{\partial y} = 0 \quad (10)$$

$$\delta \mathrm{Re}\left(u\frac{\partial u}{\partial x} + v\frac{\partial u}{\partial y}\right) = -\frac{\partial p}{\partial x} + \left(\delta^2 \frac{\partial^2 u}{\partial x^2} + \frac{\partial^2 u}{\partial y^2}\right) + g_t\theta + g_c\phi \quad (11)$$

$$\delta^3 \mathrm{Re}\left(u\frac{\partial v}{\partial x} + v\frac{\partial v}{\partial y}\right) = -\frac{\partial p}{\partial y} + \delta^2\left(\delta^2 \frac{\partial^2 v}{\partial x^2} + \frac{\partial^2 v}{\partial y^2}\right) \quad (12)$$

$$\delta\left(u\frac{\partial \theta}{\partial x} + v\frac{\partial \theta}{\partial y}\right) = \frac{1}{\mathrm{Re}\,P_r}\left\{\delta^2 \frac{\partial^2 \theta}{\partial x^2} + \frac{\partial^2 \theta}{\partial y^2}\right\} + \frac{D_f}{\mathrm{Re}}\left\{\delta^2 \frac{\partial^2 \phi}{\partial x^2} + \frac{\partial^2 \phi}{\partial y^2}\right\} \quad (13)$$

$$\delta\left(u\frac{\partial \phi}{\partial x} + v\frac{\partial \phi}{\partial y}\right) = \frac{1}{\mathrm{Re}\,S_c}\left\{\delta^2 \frac{\partial^2 \phi}{\partial x^2} + \frac{\partial^2 \phi}{\partial y^2}\right\} + \frac{S_r}{\mathrm{Re}}\left\{\delta^2 \frac{\partial^2 \theta}{\partial x^2} + \frac{\partial^2 \theta}{\partial y^2}\right\} \quad (14)$$

Introducing the dimensionless stream function $\psi(x, y)$ such that:

$$u = \frac{\partial \psi}{\partial y} \quad \text{and} \quad v = -\frac{\partial \psi}{\partial x} \quad (15)$$

The compatibility equations, which govern the problem in terms of the stream function $\psi(x, y)$ after eliminating the pressure gradient, Eqs. (11)-(14) become:

$$\mathrm{Re}\,\delta\left[(\psi_y\psi_{xyy} - \psi_x\psi_{yyy}) + \delta^2(\psi_y\psi_{xxx} - \psi_x\psi_{xxy})\right] = 2\delta^2\psi_{xxyy} + \delta^4\psi_{xxxx} + \psi_{yyyy} + g_t\theta_y + g_c\phi_y \quad (16)$$

$$\delta[\psi_y\theta_x - \psi_x\theta_y] = \frac{1}{\mathrm{Re}\,P_r}(\delta^2\theta_{xx} + \theta_{yy}) + \frac{D_f}{\mathrm{Re}}(\delta^2\phi_{xx} + \phi_{yy}) \quad (17)$$

$$\delta[\psi_y\phi_x - \psi_x\phi_y] = \frac{1}{\mathrm{Re}\,S_c}(\delta^2\phi_{xx} + \phi_{yy}) + \frac{S_r}{\mathrm{Re}}\left(\delta^2\theta_{xx} + \theta_{yy}\right) \quad (18)$$

Since we are considering the slip condition, the corresponding boundary conditions will be [35]:

$$\psi = \frac{q}{2}\ \ \psi_y + L\psi_{yy} = -1\ \ \theta = 1\ \ \phi = 1 \text{ at } y = h_1 \quad (19)$$

$$\psi = -\frac{q}{2}\ \ \psi_y - L\psi_{yy} = -1\ \ \theta = n\ \ \phi = m \text{ at } y = h_2 \quad (20)$$

where L is the non-dimensional slip parameter and q is the flux in wave frame. It should be noted that Eq. (11) for the axial pressure gradient becomes:

$$\mathrm{Re}\,\delta\left[\left(\psi_y\frac{\partial}{\partial x} - \psi_x\frac{\partial}{\partial y}\right)\psi_y\right] = -\frac{\partial p}{\partial x} + \left(\delta^2\frac{\partial^2}{\partial x^2} + \frac{\partial^2}{\partial y^2}\right)\psi_y + g_t\theta + g_c\phi \quad (21)$$

In laboratory frame, the dimensional volume flow rate is:

$$Q = \int_{H_2(X,t)}^{H_1(X,t)} U(X,Y,t)\,\mathrm{d}Y \tag{22}$$

in which H_1 and H_2 are function of X and t. The above expression in wave frame becomes:

$$q = \int_{h_2(x)}^{h_1(x)} u(x,y)\,\mathrm{d}y \tag{23}$$

where h_1 and h_2 are functions of x alone. From Eqs. (8), (22) and (23) we can write:

$$Q = q + ch_1(x) - ch_2(x) \tag{24}$$

The time-averaged flow over a period T_* at a fixed position X is:

$$\overline{Q} = \frac{1}{T_*}\int_0^{T_*} Q\,\mathrm{d}t \tag{25}$$

Substituting (24) into (25) and integrating, we get:

$$\overline{Q} = q + cd_1 + cd_2 \tag{26}$$

If we find the dimensionless mean flows Θ, in the laboratory frame, and F, in the wave frame, according to:

$$\Theta = \frac{\overline{Q}}{cd_1}, F = \frac{q}{cd_1} \tag{27}$$

one finds that Eq. (26) becomes:

$$\Theta = F + 1 + d \tag{28}$$

in which:

$$F = \int_{h_2}^{h_1} \frac{\partial \psi}{\partial y}\,\mathrm{d}y \tag{29}$$

We note that $h_1(x)$ and $h_2(x)$ represent the dimensionless form of the surfaces of the peristaltic walls:

$$\begin{aligned} h_1(x) &= 1 + a\cos(2\pi x), \\ h_2(x) &= -d - b\cos(2\pi x + \varphi) \end{aligned} \tag{30}$$

where a, b, d and φ satisfies the relation:

$$a^2 + b^2 + 2ab\cos\varphi \le (1+d)^2 \tag{31}$$

Solutions

We seek perturbation solution in terms of the small parameter δ as follows:

$$f = f_0 + \delta f_1 + \delta^2 f_2 + \ldots \tag{32}$$

where f represents any flow variable, *i.e.*,:

$$\begin{aligned} \psi &= \psi_0 + \delta\psi_1 + \delta^2\psi_2 + \ldots \\ \theta &= \theta_0 + \delta\theta_1 + \delta^2\theta_2 + \ldots \\ \phi &= \phi_0 + \delta\phi_1 + \delta^2\phi_2 + \ldots \\ p &= p_0 + \delta p_1 + \delta^2 p_2 + \ldots \end{aligned} \tag{33}$$

Substituting Eq. (33) in Eqs. (16)-(18) and collecting the coefficients of various powers of δ, we get:

The zeroth order equations are:

$$\psi_{0yyyy} + g_t\theta_{0y} + g_c\phi_{0y} = 0 \tag{34}$$

$$\frac{1}{\mathrm{Re}\,P_r}\theta_{0yy} + \frac{D_f}{\mathrm{Re}}\phi_{0yy} = 0 \tag{35}$$

$$\frac{1}{\mathrm{Re}\,S_c}\phi_{0yy} + \frac{S_r}{\mathrm{Re}}\theta_{0yy} = 0 \tag{36}$$

$$p_{0x} = \psi_{0yyy} + g_t\theta_0 + g_c\phi_0 \tag{37}$$

The corresponding dimensionless boundary conditions in the wave frame are:

$$\psi_0 = \frac{q}{2}\ \ \psi_{0y} + L\psi_{0yy} = -1\ \ \theta_0 = 1\ \ \phi_0 = 1 \text{ at } y = h_1 \tag{38}$$

$$\psi_0 = -\frac{q}{2}\ \ \psi_{0y} - L\psi_{0yy} = -1\ \ \theta_0 = n\ \ \phi_0 = m \text{ at } y = h_2 \tag{39}$$

The first order equations are:

$$\mathrm{Re}[\psi_{0y}\psi_{0xyy} - \psi_{0x}\psi_{0yyy}] = \psi_{1yyyy} + g_t\theta_{1y} + g_c\phi_{1y} \tag{40}$$

$$\psi_{0y}\theta_{0x} - \psi_{0x}\theta_{0y} = \frac{1}{\mathrm{Re}\,P_r}\theta_{1yy} + \frac{D_f}{\mathrm{Re}}\phi_{1yy} \tag{41}$$

$$\psi_{0y}\phi_{0x} - \psi_{0x}\phi_{0y} = \frac{1}{\mathrm{Re}\,\mathrm{S_c}}\phi_{1yy} + \frac{\mathrm{S_r}}{\mathrm{Re}}\theta_{1yy} \tag{42}$$

$$p_{1x} = \psi_{1yyy} + g_t\theta_1 + g_c\phi_1 - \mathrm{Re}[\psi_{0y}\psi_{0xy} - \psi_{0x}\psi_{0yy}] \tag{43}$$

The corresponding dimensionless boundary conditions in the wave frame are:

$$\psi_1 = 0\ \ \psi_{1y} + L\psi_{1yy} = 0\ \ \theta_1 = 0\ \ \phi_1 = 0 \text{ at } y = h_1 \tag{44}$$

$$\psi_1 = 0\ \ \psi_{1y} - L\psi_{1yy} = 0\ \ \theta_1 = 0\ \ \phi_1 = 0 \text{ at } y = h_2 \tag{45}$$

Solving the Eqs. (34)-(36) with boundary conditions (38) and (39) and the Eqs. (40)-(42) with boundary conditions (44) and (45), we get:

Zeroth order solution:

$$\theta_0 = A + By \tag{46}$$

$$\phi_0 = \mathrm{A}_1 + B_1 y \tag{47}$$

$$\psi_0 = A_2 + B_2 y + C_2 y^2 + D_2 y^3 + T_2 y^4 \tag{48}$$

$$p_{0x} = (g_t B + g_c B_1 + 24T_2)\, y + 6D_2 + g_t A + g_c A_1 \quad (49)$$

First order solution:

$$\theta_1 = A_3 + B_3 y + T_{24} y^2 + T_{25} y^3 + T_{26} y^4 + T_{27} y^5 + T_{28} y^6 \quad (50)$$

$$\phi_1 = A_4 + B_4 y + T_{42} y^2 + T_{43} y^3 + T_{44} y^4 + T_{45} y^5 + T_{46} y^6 \quad (51)$$

$$\psi_1 = A_5 + B_5 y + C_5 y^2 + D_5 y^3 + T_{65} y^4 + T_{66} y^5 + T_{67} y^6 + T_{68} y^7 + T_{69} y^8 + T_{70} y^9 \quad (52)$$

$$p_{1x} = T_{91} + T_{92} y + T_{93} y^2 + T_{94} y^3 + T_{95} y^4 + T_{96} y^5 + T_{97} y^6 \quad (53)$$

The pressure rise per wavelength is denoted by Δp_λ and defined as follows:

$$\Delta p_\lambda = \int_0^1 \left(\frac{\partial p}{\partial x} \right) \mathrm{d}x \quad (54)$$

The frictional forces at y = h_1 and y = h_2, denoted by $F_{\lambda 1}$ $F_{\lambda 2}$, respectively, are given as:

$$F_{\lambda 1} = \int_0^1 -h_1^2 \left(\frac{\mathrm{d}p}{\mathrm{d}x} \right) \mathrm{d}x \quad (55)$$

$$F_{\lambda 2} = \int_0^1 -h_2^2 \left(\frac{\mathrm{d}p}{\mathrm{d}x} \right) \mathrm{d}x \quad (56)$$

The coefficient of heat transfer at the wall is given by

$$Z = h_{2x}\theta_{0y} + \delta\left(\theta_{0x} + h_{2x}\theta_{1y}\right) \quad (57)$$

The shearing stress acting on the (left and right) wall is defined as:

$$\bar{\tau} = \frac{\sigma_{xy}\left\{1 - \left(\frac{dy}{dx}\right)^2\right\} + \left(\sigma_{yy} - \sigma_{xx}\right)\left(\frac{dy}{dx}\right)}{1 + \left(\frac{dy}{dx}\right)^2} \quad (58)$$

at $y = H_2(x)$ and $H_1(x)$

where $\sigma_{xy}, \sigma_{yy}, \sigma_{xx}$ are the usual stress components.

The non-dimensional shear stress reduces to:

$$\tau = 2C_2 + 6D_2 y + 12T_2 y^2 + \delta(2C_5 + 6D_5 y + 12T_{65} y^2 + 20T_{66} y^3 + 30T_{67} y^4 + 42T_{68} y^5 + 56T_{69} y^6 + 72T_{70} y^7) \quad (59)$$

RESULTS AND DISCUSSION

The effect of various parameters on velocity is plotted in Figure 2. It shows that the amplitude of the velocity increases with an increase of q, D_f and φ. While it decreases with an increase of L. Further we note that when q = -2 and L is increased from 0 to 0.1 there is approximately 6.25% decrease of velocity, which shows that the slip parameter affects the flow field significantly.

Figure 3 shows the dimensionless pressure change per wavelength (Δp_λ) *versus* the dimensionless flow rate (Θ). The graph is sectored so that the upper right hand quadrant (I) denotes the region of peristaltic pumping where $\Theta > 0$ (positive pumping) and $\Delta p_\lambda > 0$ (adverse pressure gradient). Quadrant II, where $\Delta p_\lambda < 0$ (favorable pressure gradient) and $\Theta > 0$ (positive pumping), is designated as augmented flow. Quadrant IV such that $\Delta p_\lambda > 0$ (adverse pressure gradient) and $\Theta < 0$ is called retrograde or backward pumping. The flow is opposite to the direction of the peristaltic motion. Figure 3a is plotted to see the effect of g_t on Δp_λ *versus* Θ. We observe that an increase in g_t increases the peristaltic pumping rate (for the same Δp_λ). Figure 3b is graphed to see the effect of n on Δp_λ. It is observed that the pumping rate increases with the increase of n. A similar result is shown in Figure 3c if n is replaced by φ. Figure 3d depicts that increasing slip parameter leads to decrease the pumping region.

Figure 4 illustrates frictional force at wall $y = h_1$ *versus* dimensionless average volume flow rate Θ for different values of g_t and n. The effects of these parameters on the frictional force are quite opposite to that of pumping characteristics. Figure 5 shows that variation of φ and L on frictional force (at right wall y = h_2 of the channel) *versus* flow rate Θ. It is clear that the influence of q and L on $F_{\lambda 2}$ is similar to that of g_t and n on $F_{\lambda 1}$.

Figure 6 was plotted to see the effect of L, q, φ and n on the pressure gradient. It shows that the pressure gradient decreases with the increase of L, q and φ while it increases with increasing n. Further, we may note that in the wider part of the channel $x \in [0, 0.25]$ and $x \in [0.7, 1]$, the pressure gradient (variation) is very small and in the narrow part of the channel $x \in [0.25, 0.7]$, dp/dx increases (Figure 6d).

Figure 7 displays the temperature profiles for various values of D_f and P_r. The behavior of the fluid temperature with changing D_f is shown in Figure 7a. This shows that temperature decreases with an increase of D_f. In Figure 7b, we note that increasing P_r leads to increase the fluid temperature. The aim of Figure 8 is to examine the fluid concentration for different values of P_r and Re. Figure 8a is prepared to see the influence of P_r on concentration field. It shows that there is decrease in the concentration distribution with increasing P_r. Similar effects can be found for the be-

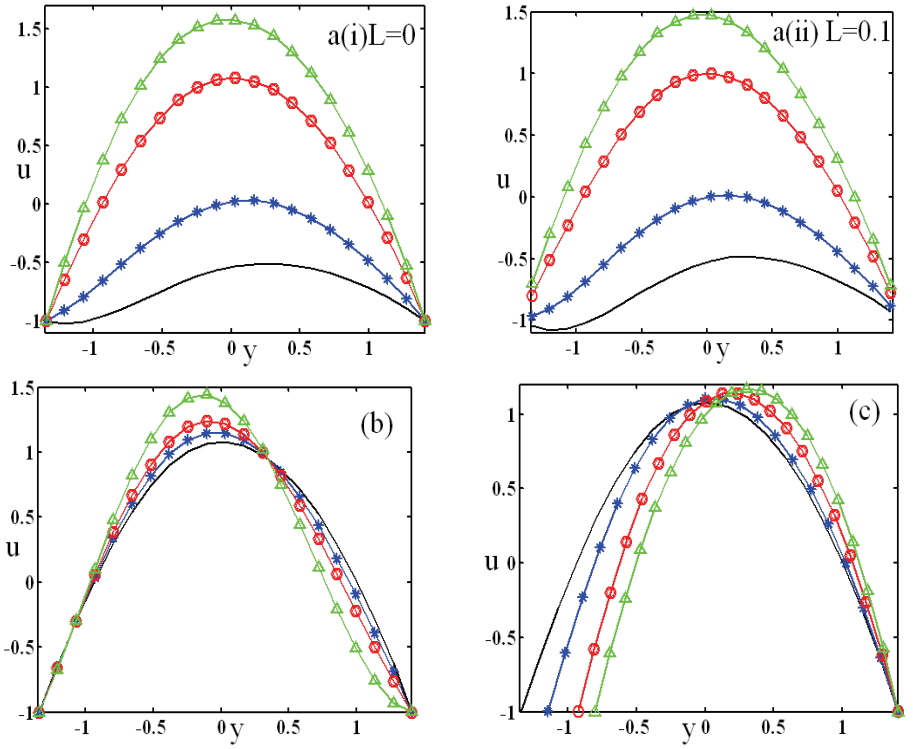

Figure 2. Velocity distribution; a = 0.5, b = 0.3, d = 1.1, x = 0.1, m = 2, n = -1, S_c = 0.5, S_r = 0.5, g_c = 5, g_t = 5,P_r = 0.71, δ = 0.01; a) (–) q = -2, (✳) q = -1, (○) q = 1, (Δ) q = 2, D_f = 0.05, φ = 0, Re = 7, b) (–) D_f = 0.05, (✳) D_f = 1, (○) D_f = 1.5, (Δ) D_f = 2, q = 1, φ = 0, Re = 7, L = 0, c) (–) φ = 0, (✳) φ = π/4, (○) φ = π/2, (Δ) φ = 3π/4, q = 1, D_f = 0.05, Re = 7, L = 0.

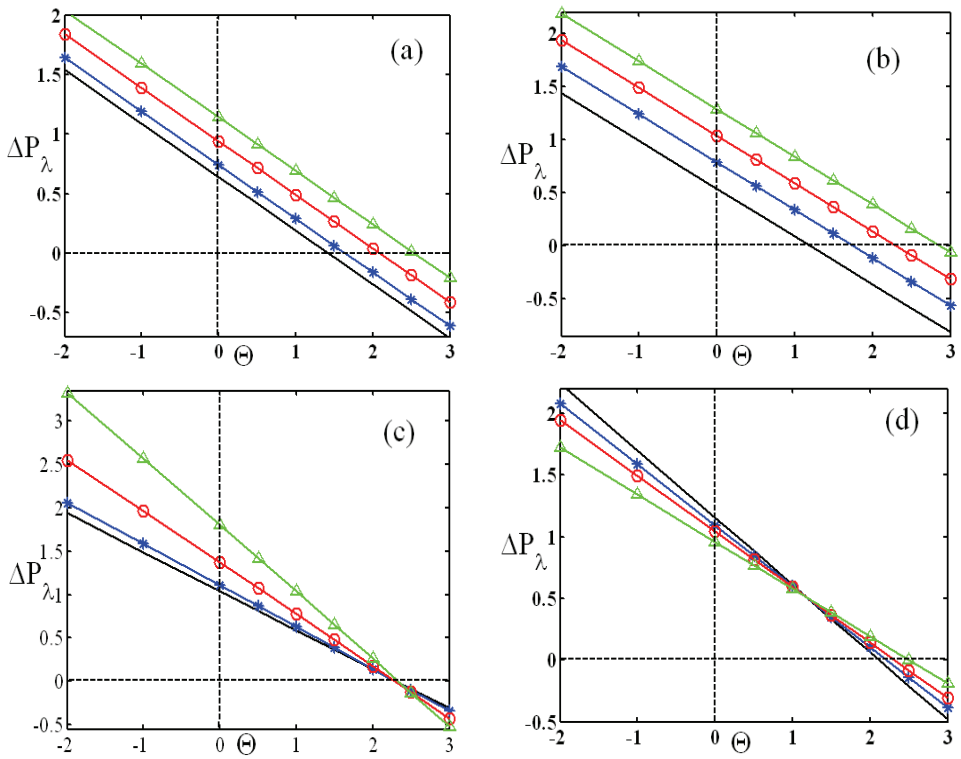

Figure 3. Pressure drop; a = 0.5, b = 0.3, d = 1.1, x = 0.1, m = -1, S_c = 0.5, S_r = 0.5, g_c = 5, P_r = 0.71, δ = 0.01, Re = 2, D_f = 0.05; a) (–) g_t = 0.1, (✳) g_t = 0.2, (○) g_t = 0.4, (Δ) g_t = 0.6, n = 1, φ = 0, L = 0.1; b) (–) n = -1, (✳) n = 0, (○) n = 1, (Δ) n = 2, φ = 0, L = 0.1, g_t = 0.5; c) (–) φ = 0, (✳) φ = π/4, (○) φ = π/2, (Δ) φ = 3π/4, n = 1, L = 0.1, g_t = 0.5; d) (–) L = 0, (✳) L = 0.05, (○) L = 0.1, (Δ) L = 0.2, n = 1, φ = 0, g_t = 0.5.

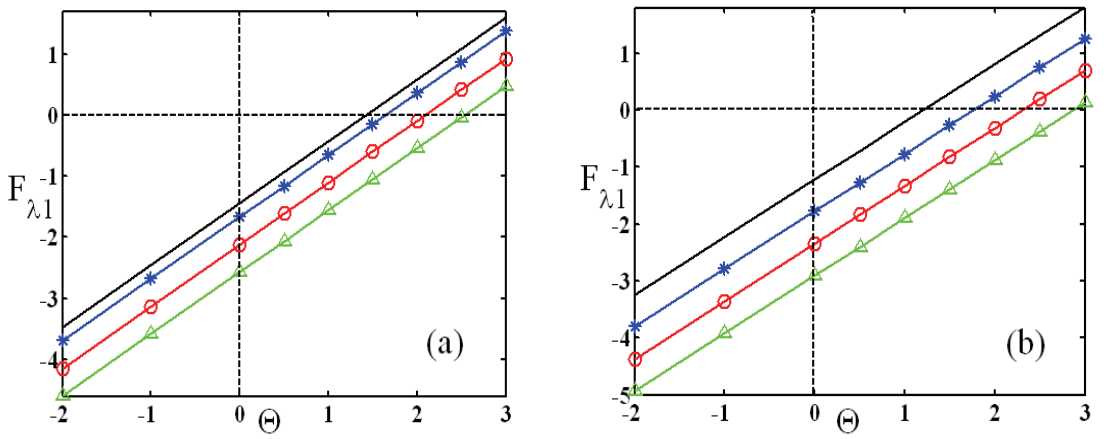

Figure 4. Frictional Forces at the wall $y = h_1$; $a = 0.5$, $b = 0.3$, $d = 1.1$, $x = 0.1$, $m = -1$, $S_c = 0.5$, $S_r = 0.5$, $g_c = 5$, $P_r = 0.71$, $\delta = 0.01$, $Re = 2$, $D_f = 0.05$, $\varphi = 0$, $L = 0.1$; a) (–) $g_t = 0.1$, (✳) $g_t = 0.2$, (○) $g_t = 0.4$, (Δ) $g_t = 0.6$, $n = 1$; b) (–) $n = -1$, (✳) $n = 0$, (○) $n = 1$, (Δ) $n = 2$, $g_t = 0.5$.

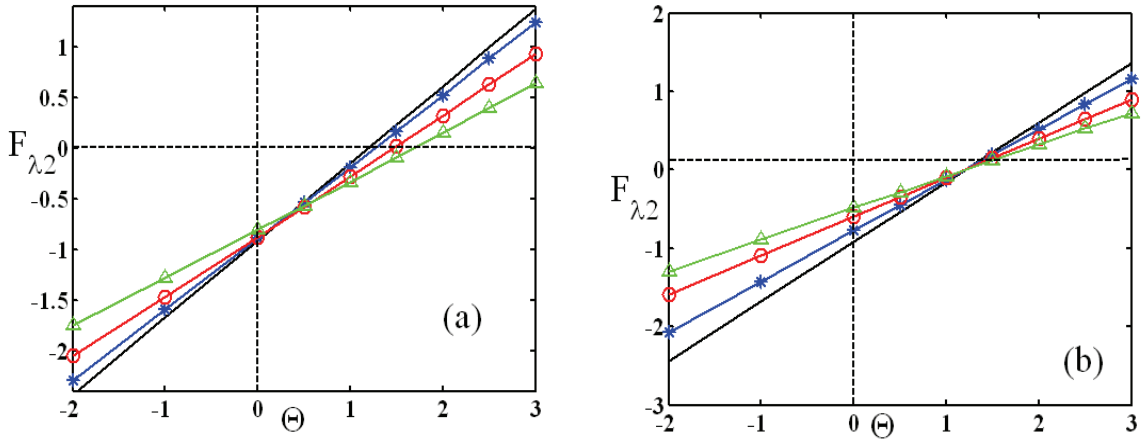

Figure 5. Frictional Forces at the wall $y = h_2$; $a = 0.5$, $b = 0.3$, $d = 1.1$, $x = 0.1$, $n = -1$, $m = -1$, $S_c = 0.5$, $S_r = 0.5$, $g_c = 5$, $g_t = 5$, $P_r = 0.71$, $\delta = 0.01$, $Re = 2$, $D_f = 0.05$; a) (–) $\varphi = 0$, (✳) $\varphi = \pi/4$, (○) $\varphi = \pi/2$, (Δ) $\varphi = 3\pi/4$, $L = 0.1$; b) (–) $L = 0$, (✳) $L = 0.05$, (○) $L = 0.1$, (Δ) $L = 0.2$, $\varphi = 0$.

havior of concentration distribution for different values of Re, which is shown in Figure 8b.

Figure 9 is prepared to see the role of different values of Re, D_f, P_r and g_t on shear stress distribution. We notice that stress is in oscillatory behavior, which may be due to peristalsis. Further, we observe that when $x < 0$ shear stress decreases with increasing Re, D_f and g_t while it increases with increasing P_r but this behavior is reversed, when $x > 0$. The effects of L, P_r, φ and g_t on the coefficient of heat transfer is analyzed through Figure 10. From these figures, we observe that the heat transfer coefficient increases by increasing φ and g_t but the opposite effect could be noticed with increasing L and P_r.

CONLCLUSION

The problem of mixed convective heat and mass transfer peristaltic flow in a vertical asymmetric channel with wall slip has been analyzed. The momentum and energy equations have been linearized under long-wavelength approximation. Analytical solutions have been constructed for stream function, temperature, concentration and heat transfer coefficient. The features of the flow characteristics are analyzed for various values of involved parameters and discussed. It is observed that velocity decreases with an increase of the slip parameter. The pumping rate increases with the increase of Grashof number and phase difference while it reduces with increasing slip. The pressure gradient decreases with the increase of the slip parameter. Furthermore, the heat transfer coefficient decreases with the increase of the slip parameter and Prandtl number.

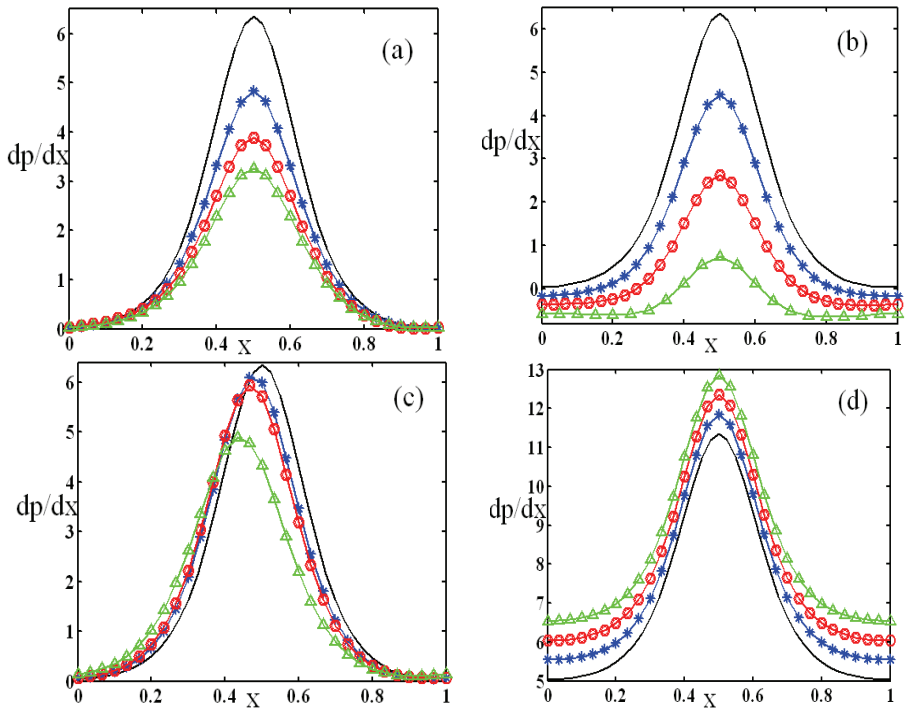

Figure 6. Pressure gradient; a = 0.5, b = 0.3, d = 1.1, x = 0.1, m = -1, S_c = 0.5, S_r = 0.5, g_c = 5, g_t = 5, P_r = 0.71, D_f = 0.5, Re = 1 δ = 0.001; a) (–) L = 0.1, (✳) L = 0.2, (○) L = 0.3, (Δ) L = 0.4, q = -3, n = -1, φ = 0; b) (–) q = -3, (✳) q = -2.5, (○) q = -2, (Δ) q = -1.5, L = 0.1, n = -1, φ = 0; c) (–) φ = 0, (✳) φ = π/8, (○) φ = π/6, (Δ) φ = π/3, L = 0.1, q = -3, n = -1; d) (–) n = 1, (✳) n = 1.2, (○) n = 1.4, (Δ) n = 1.6, L = 0.1, q = -3, φ = 0.

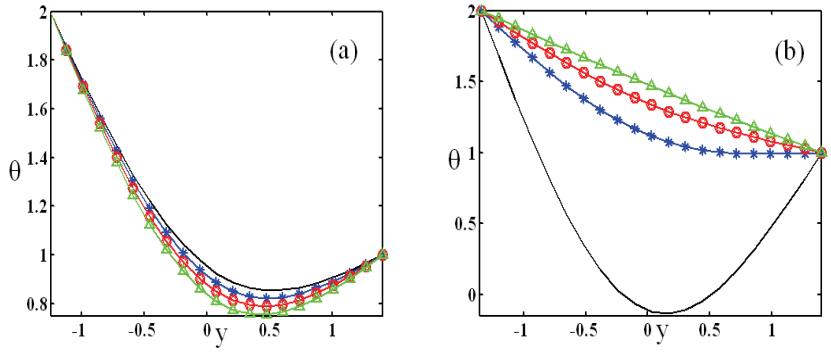

Figure 7. Temperature distribution; a = 0.5, b = 0.3, d = 1.1, x = 0.1, n = 2, m = -2, q = -1, S_c = 0.2, S_r = 0.2, g_c = 5, g_t = 5, δ = 0.3, Re = 7, φ = 0, L = 0.1; a) (–) D_f = 0, (✳) D_f = 0.1, (○) D_f = 0.2, (Δ)D_f = 0.3, P_r = 0.71; b) (–) P_r = 0.71, (✳)P_r = 1, (○) P_r = 7, (Δ)P_r = 11.4, D_f = 0.01.

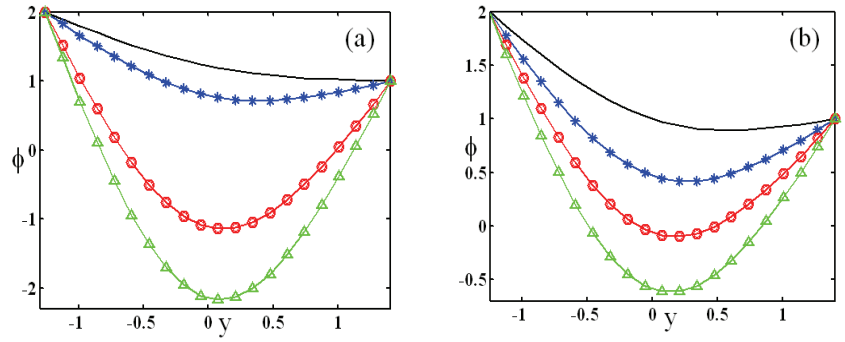

Figure 8. Concentration distribution; a = 0.5, b = 0.3, d = 1.1, x = 0.1, n = -2, m = 2, q = 1, S_c = 0.2, S_r = 0.2, g_c = 5, g_t = 5, δ = 0.2, Re = 7, φ = π/8, D_f = 0.05, L = 0.1; a) (–) P_r = 0.044, (✳)P_r = 1, (○) P_r = 5, (Δ)P_r = 7, Re = 5, b) (–) Re = 1, (✳) Re = 2, (○) Re = 3, (Δ) Re = 4, P_r = 5.

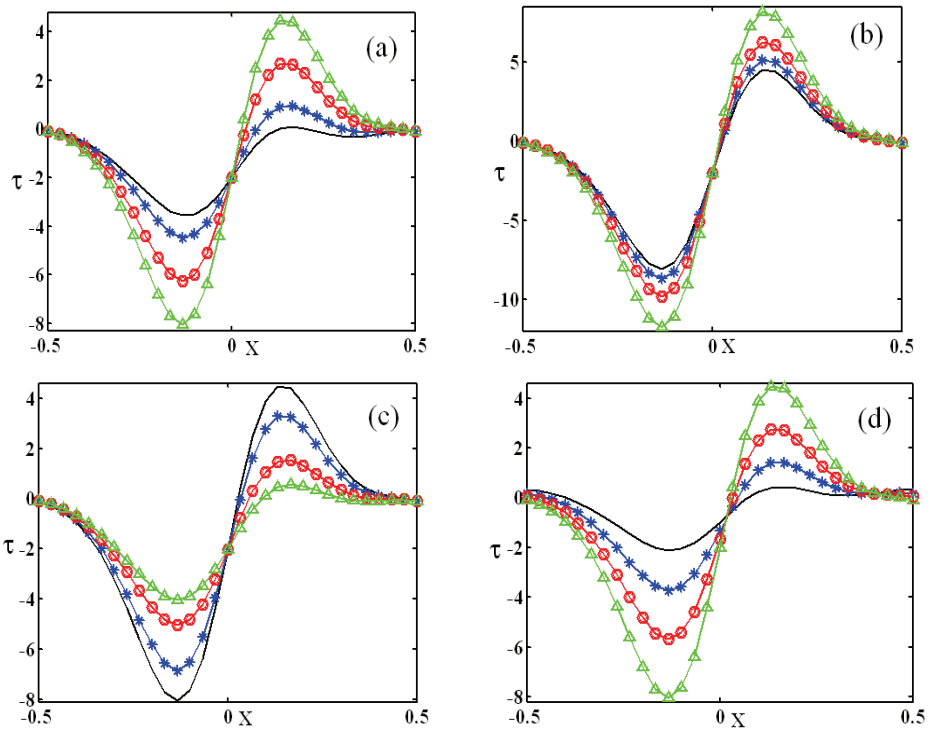

Figure 9. Shear stress distribution; a = 0.3, b = 0.4, d = 1.1, x = 0.1, n = -1, m = 1, q = -2, S_c = 0.2, S_r = 0.2, g_c = 5, g_t = 5, δ = 0.3, φ = 0, L = 0.1; a) (–) Re = 2, (✳) Re = 3, (○) Re = 5, (Δ) Re = 7, D_f = 0.05, P_r = 0.71, g_t = 5; b) (–) D_f = 0.05, (✳) D_f = 0.5, (○) D_f = 1, (Δ) D_f = 1.5, Re = 7, P_r = 0.71, g_t = 5; c) (–) P_r = 0.71, (✳) P_r = 1, (○) P_r = 2, (Δ) P_r = 3, Re = 7, D_f = 0.05, g_t = 5; d) (–) g_t = 2, (✳) g_t = 3, (○) g_t = 4, (Δ) g_t = 5, Re = 7, D_f =0.05, P_r = 0.71.

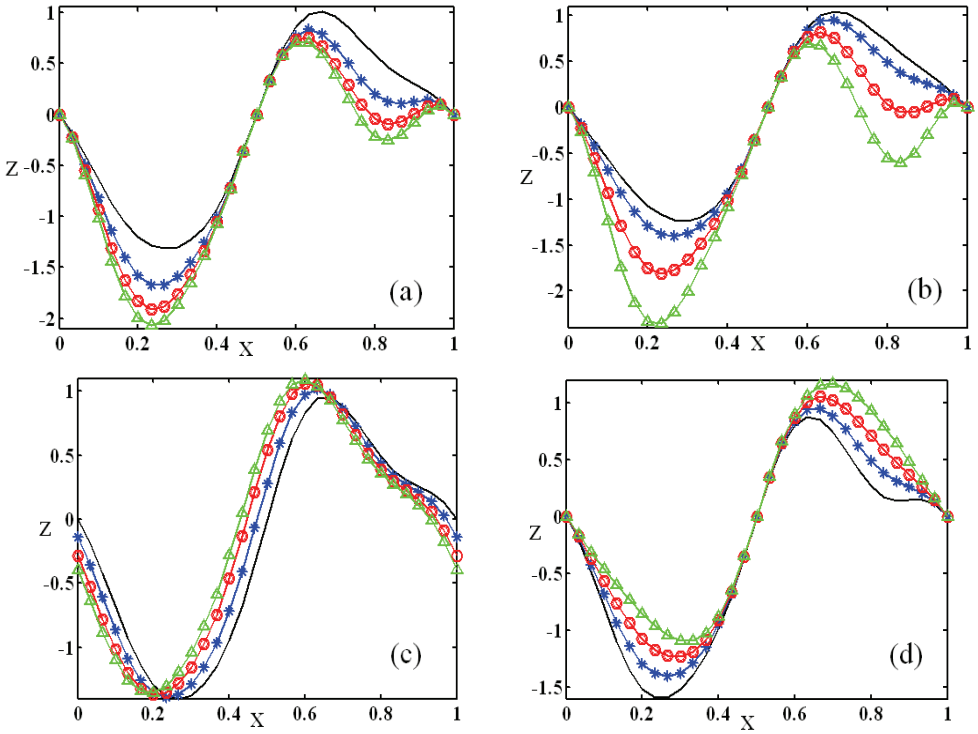

Figure 10. Coefficient of heat transfer; a = 0.5, b = 0.3, d = 1.1, x = 0.1, n = 2, m = -2, q = 1, S_c = 5, S_r = 5, g_c = 5, δ = 0.1, Re = 1, D_f = 0.05; a) (–) L = 0, (✳) L = 0.5, (○) L = 1, (Δ) L = 1.5, P_r = 0.71, φ = 0, g_t = 5; b) (–) P_r = 0.044, (✳) P_r = 0.71, (○) P_r = 1, (Δ) P_r = 1.1, L = 0.1, φ = 0 , g_t = 5; c) (–) φ = 0, (✳) φ = π/16, (○) φ = π/8, (Δ) φ = π/6, L = 0.1, P_r = 0.71, g_t = 5; d) (–) g_t = 0, (✳) g_t = 5, (○) g_t = 10, (Δ) g_t = 15,L = 0.1, P_r = 0.71, φ = 0.

Acknowledgement

Authors acknowledge the financial support from Department of Science and Technology, Govt. of India under the project number SR/S4.MS:674/10.

Nomenclature

a_1, b_1 - The amplitudes of the waves
C_0, C_1 - Wall concentrations
$\bar{C}$ - The concentration at some reference point
C - Species concentration
c_p - Specific heat at constant pressure
c_s - The concentration susceptibility
D_m - Coefficient of mass diffusivity
D_f - Dufour number
$d_1 + d_2$ - The width of the channel
L - Non-dimensional slip parameter
g_t - Grashof number
g_c - Local mass Grashof number
g - Gravitational acceleration
k_T - Thermal diffusion ratio
k - Thermal conductivity
p - Pressure
P_r - Prandtl number
Re - Reynolds number
S_c - Schmidt number
S_r - Soret number
T - Temperature distribution
T_0, T_1 - Wall temperatures
$\bar{T}$ - The temperature at some reference point
U, V - The velocity components in X and Y direction
u, v - The velocity components in x and y direction

Greek symbols

β_c - Concentration expansion coefficient
β_t - Thermal expansion coefficient
μ - Dynamic viscosity
θ - Non dimensional temperature distribution
ρ - Density of the fluid
φ - Phase difference
ϕ - Non dimensional concentration
δ - Dimensionless wave number
λ - The wave length
ψ - Non-dimensional stream function
$\bar{\tau}, \tau$ - Dimensional and non-dimensional shear stress.

REFERENCES

[1] L.N. Tao, ASME J. Heat Transfer. **82** (1960) 233-238
[2] W. Aung, G. Worku, ASME J. Heat Trans. **108** (1986) 485-488
[3] A. Barletta, Int. J. Heat Mass Trans. **42** (1999) 3501-3513
[4] A.J. Chamkha, T. Grosan, I. Pop, Int. Comm. Heat Mass Trans. **29** (2002) 1119-1127
[5] J. Prathap Kumar, J.C. Umavathi, I. Pop, B.M. Biradar, Trans. porous media **80** (2009) 117-135
[6] I. Pop, T. Grosan, R. Cornelia, Commun. Non Linear Sci. Numer. Simul. **15** (2010) 471-474
[7] R. Muthuraj, S. Srinivas, Comput. Math. Appl. **59** (2010) 3516-3528
[8] T.W. Latham, MS Thesis, MIT Cambridge, 1966
[9] O. Eytan, D. Elad, Bull. Math. Bio. **61**(1999) 221
[10] M. Mishra, A. Ramachandra Rao, ZAMP **54** (2003) 532--550
[11] Kh.S. Mekheimer, Appl. Math. Comput. **153** (2004) 763--777
[12] M.V. Subba Reddy, A. Ramachandra Rao, S. Sreenath, Int. J. Non-linear Mech. **42** (2007) 1153 -1161
[13] M. Kothandapani, S. Srinivas, Phys. Lett., A **372**(2008) 1265-1276
[14] Kh. S. Mekheimer, Phys. Lett., A **372** (2008) 4271-4278
[15] N. Ali, T. Hayat, S. Asghar, Chaos Solitons Fractals **39** (2009) 407-416
[16] R. Ellahi, Commun. Nonlinear Sci. Numer. Simul. **14** (2009) 1377-1384
[17] G. Radhakrishnamacharya, V. Radhakrishna Murthy, Def. Sci. J. **43** (1993) 275-280
[18] K. Vajravelu, G. Radhakrishnamacharya, V. Radhakrishnamurty, Int. J. Non Linear Mech. **42** (2007) 754-759
[19] Kh. S. Mekheimer, Y. Abd Elmaboud, Phys. Lett., A **372** (2008) 1657-1665
[20] T. Hayat, M.U. Qureshi, Q. Hussain, Appl. Math. Model. **33** (2009) 1862-1873
[21] N.T.M. Eldabe, M.F. El-Sayed, A.Y. Ghaly, H.M. Sayed, Archi. Appl. Mech. **78** (2007) 599-624
[22] S. Srinivas, M. Kothandapani, Appl. Math. Comput. **213** (2009) 197-208
[23] S. Nadeem, S. Akram, Commun. Nonlinear Sci. Numer. Simul. **15** (2010) 312-321
[24] S. Nadeem, S. Akram, Z. Naturforsch. **65a** (2010) 483-494
[25] S. Nadeem, S. Akram, Int. J. Numer. Methods Fluids **63** (2010) 374-394
[26] S. Nadeem, S. Akram, Commun. Non Linear Sci. Numer. Simul. **15** (2010) 1705-1716
[27] T. Hayat, S. Hina, Non linear Anal. Real World Appl. **11** (2010) 3155-3169
[28] S. Nadeem, N. Akbar, J. Taiwan Inst. Chem. Eng. **41** (2010) 286-294
[29] S. Srinivas, R. Gayathri, M. Kothandapani, Commun. Non Linear Sci. Numer. Simul.**16** (2011) 1845-1862
[30] S. Srinivas, R. Muthuraj, Math. Comput. Model. **54** (2011) 1213-1227
[31] S. Nadeem, N.S. Akbar, J. Mech. Med. Biol. **11** (2011) 1--30
[32] Y. Abd Elmaboud, Kh.S. Mekheimer, Appl. Math. Model. **35** (2011) 2695-2710
[33] Kh.S. Mekheimer, S.Z.-A. Husseny, A.I. Abd el Lateef, Appl. Bionics Biomech. **8** (2011) 295-308.

[34] K. S. Mekheimer, N. Saleem, T. Hayat, A. A. Hendi, Int. J. Numer. Methods Fluids (2011), doi: 10.1002/fld.2693 2011

[35] Kh. S. Mekheimer, A. N. Abdel-Wahab, J. Aerospace Eng. (2011), doi: 10.1061/(ASCE)AS.1943-5525.0000151

[36] C.L.M.H. Navier, Mem. Acad. R. Sci. Inst. France **1**(1823) 414-421

[37] J. Happel, H. Brenner, Low Reynolds number Hydrodynamics, Kluwer, Boston, MA, 1983

[38] I.J. Rao, K.R. Rajagopal, Acta Mech. **135** (1999) 113-126

[39] T. Rajeev, N.C. Jain, Def. Sci. J. **54** (2004) 21-29

[40] E.F. El-Shehawy, N.T. El-Dabe, I.M. El-Desoky, Acta Mech. **186** (2006) 141-159

[41] T. Hayat, M. Qureshi, N. Ali, Phys. Lett., A **372** (2007) 2653-2664

[42] J. Hron, C.L. Roux, J. Malik, K.R. Rajagopal, Comput. Math. Appl. **56** (2008) 2128-2143

[43] N. Ali, Q. Hussain, T. Hayat, S. Asghar, Phys. Lett., A **372** (2008) 1477-1489

[44] A. Ebaid, Phys. Lett., A **372** (2008) 4493-4499

[45] S. Srinivas, R. Gayathri, M. Kothandapani, Comput. Phys. Commun. **180** (2009) 2115-2122

[46] S. Srinivas, R. Muthuraj, Chem. Eng. Commun. **197** (2010) 1387-1403.

S. SRINIVAS[1]
R. MUTHURAJ[2]
J. SAKINA[1]

[1]Fluid Dynamics Division, School of Advanced Sciences, VIT University, Vellore, India
[2]Department of Mathematics, P.S.N.A. College of Engineering and Technology, Dindigul, India

NAUČNI RAD

O UTICAJU PRENOSA MASE I TOPLOTE NA PERISTALTIČKO STRUJANJE VISKOZNOG FLUIDA KROZ VERTIKALNI ASIMETRIČNI KANAL SA KLIZANJEM PO ZIDU

Ovaj rad se bavi uticajem prenosa mase i toplote na peristaltičko strujanje viskoznog fluida u uslovima klizanja po zidu. Ovo strujanje je ispitivano u talasnom okviru reference koja se kreće sa brzinom talasa. Asimetrija kanala se stvara izborom peristaltičkog talasnog voza na zidovima da bi se postigle različite amplitude i faze. Jednačine bilansa količine kretanja i energije su linearizovane pod pretpostavkom pretpostavkom velike talasne dužine. Izvedene jednačine su rešene tehnikom perturbacije i dobijeni su izrazi za promene temperature, koncentracije, brzine i strujne funkcije. Rezultati su prikazani grafički za različite parametre, a zatim diskutovani.

Ključne reči: konvekcija; peristaltičko strujanje; asimetrični kanal; klizanje po zidu; Dufourov broj; Šmitov broj.